0026-895X/05/6704-992–1004$20.00
MOLECULAR PHARMACOLOGY

Mol Pharmacol 67:992–1004, 2005

Vol. 67, No. 4
8417/1197208
Printed in U.S.A.

ACCELERATED COMMUNICATION

β-Arrestin-Dependent Spontaneous α_{1a}-Adrenoceptor Endocytosis Causes Intracellular Transportation of α-Blockers via Recycling Compartments[S]

John D. Pediani, Janet F. Colston, Darren Caldwell, Graeme Milligan, Craig J. Daly, and John C. McGrath

Autonomic Physiology Unit, Division of Neuroscience and Biomedical Systems (J.D.P., J.F.C., D.C., C.J.D., J.C.M.), and Molecular Pharmacology Group, Division of Biochemistry and Molecular Biology (G.M.), Institute of Biomedical and Life Sciences, University of Glasgow, Glasgow, Scotland, United Kingdom

Received October 19, 2004; accepted December 21, 2004

ABSTRACT

The antagonist ligand BODIPY-FL-prazosin (QAPB) fluoresces when bound to bovine α_{1a}-adrenoceptors (ARs). Data indicate that the receptor-ligand complex is spontaneously internalized by β-arrestin-dependent endocytosis. Internalization of the ligand did not occur in β-arrestin-deficient cells; was blocked or reversed by another α_1 ligand, phentolamine, indicating it to reflect binding to the orthosteric recognition site; and was prevented by blocking clathrin-mediated endocytosis. The ligand showed rapid, diffuse, low-intensity, surface binding, superseded by punctate intracellular binding that developed to equilibrium in 50 to 60 min and was reversible on ligand removal, indicating a dynamic equilibrium. In cells expressing a human α_{1a}-AR-enhanced green fluorescent protein (EGFP) 2 fusion protein, BODIPY-R-558/568-prazosin (RQAPB) colocalized with the fusion, indicating that the ligand gained access to all compartments containing the receptor, and, conversely, that the receptor has affinity for the ligand at all of these sites. The distribution of QAPB binding sites was similar for receptors with or without EGFP2, validating the fusion protein as an indicator of receptor location. The ligand partially colocalized with β-arrestin in recycling and late endosomes, indicating receptor transit without destruction. Organelles containing receptors showed considerable movement consistent with a transportation function. This was absent in β-arrestin-deficient cells, indicating that both constitutive receptor internalization and subsequent intracellular transportation are β-arrestin-dependent. Calculations of relative receptor number indicate that at steady state, less than 30% of receptors reside on the cell surface and that recycling is rapid. We conclude that α_{1a}-ARs recycle rapidly by an agonist-independent, constitutive, β-arrestin-dependent process and that this can transport "α-blockers" into cells carrying these receptors.

We have observed in live smooth muscle cells expressing α_1-ARs that a fluorescent antagonist ligand, the prazosin analog QAPB, labels intracellular receptors. This process takes longer than expected of simple diffusion, suggesting an uptake process (Mackenzie et al., 2000). It is known that fluorescent agonists can be internalized while bound to the receptors that they activate (Kallal and Benovic, 2000, 2002; Daly and McGrath, 2003). It is also possible that antagonists of receptor-mediated second messenger regulation can initiate internalization, as shown previously for the cholecystokinin receptor (Roettger et al., 1997). However, an antagonist ligand might be internalized simply by binding to a receptor that is spontaneously recycling. Morris et al. (2004) recently showed that when expressed in rat-1 fibroblasts (R-1Fs), the

D.C. was supported by a Medical Research Council Ph.D. studentship and J.F.C. was supported by the Ann B. McNaught Bequest.

[S] The online version of this article (available at http://molpharm.aspetjournals.org) contains supplemental material.

Article, publication date, and citation information can be found at http://molpharm.aspetjournals.org.
doi:10.1124/mol.104.008417.

ABBREVIATIONS: α_1-AR, α_1-adrenoceptor; QAPB, BODIPY-FL prazosin; R-1F, rat-1 fibroblast; EGFP, enhanced green fluorescent protein; DMEM, Dulbecco's modified Eagle's medium; PBS, phosphate-buffered saline; Con A, concanavalin A; RQAPB, BODIPY-R 558/568 prazosin; HEK, human embryonic kidney; MEF, mouse embryo fibroblast; Tfn, transferrin; 3D, three-dimensional; 2D, two-dimensional; GFP, green fluorescent protein.

human α_{1a}-AR can internalize spontaneously by using antibodies to an extracellular epitope to follow the receptors, excluding the possibility of internalization through occupation of the receptive site.

We now show that antagonists such as QAPB can be internalized bound to spontaneously recycling α_{1a}-ARs and analyze the mechanisms involved. QAPB is a prazosin analog in which the furan ring has been substituted by a BODIPY fluorescent moiety. It retains prazosin's high affinity, functional antagonism, and relative selectivity for α_1-ARs, and, like prazosin, does not distinguish within the family of three α_1-AR subtypes. Importantly for its present use, it fluoresces when bound to the receptor in live cells, yet it remains essentially nonfluorescent in the aqueous phase. This allows quantitative visual assessment of its binding to receptors at equilibrium (Daly et al., 1998). It has been used to measure binding affinity at recombinant and native α_1-ARs in different regions of cultured cells and of freshly dissociated cells from human and other mammalian tissue (McGrath et al., 1996, 1999; Daly et al., 1998; Mackenzie et al., 2000). We have quantified the pharmacology of agonist and antagonist interaction at recombinant α_1-AR in R-1Fs (Pediani et al., 2000), demonstrating that the receptors are functional and have the predicted pharmacology. This cell line provides the main basis for the present study. We accomplished real-time visualization of antagonist-receptor binding interactions in a concentration range near to the ligand's dissociation constant. Binding was found at intracellular sites as well as on the cell surface. We further established the utility of the fluorescent ligand by demonstrating colocalization of the QAPB-receptor complex and receptors tagged with the autofluorescent green fluorescent protein variant EGFP2. These independent measures of receptor location allowed us to cross-validate the fluorescent ligand as reflecting the localization of receptor binding sites and the EGFP2 as indicating the presence of receptors that could bind antagonists. We investigated the mechanism by which the ligand entered the cell by blocking internalization processes and used vital organelle markers to identify the compartments in which the α_{1a}-AR-ligand fluorescent complex resides. Analysis of the contribution of β-arrestin indicated that α_{1a}-AR spontaneously recycle in a β-arrestin-dependent but agonist-independent manner. The rate of uptake and cellular distribution of the ligand-receptor complex were used to estimate the turnover of the spontaneous recycling process.

Materials and Methods

Materials

Cell culture plastics were supplied by Falcon (BD Biosciences Discovery Labware, Bedford, MA) or PerkinElmer Life and Analytical Sciences (Boston, MA). Dulbecco's modified Eagle's medium (DMEM) with sodium pyruvate, newborn calf serum, L-glutamine, penicillin, streptomycin, active G418 (Geneticin; 50 mg/ml), trypsin/ethylenediamine tetraacetic acid, pCDNA3, and Dulbecco's phosphate-buffered saline (PBS) were purchased from Invitrogen (Paisley, Scotland). The pEGFP2 N2 vector was purchased from PerkinElmer Life and Analytical Sciences (Berkshire, UK). HEPES, sucrose, phenylephrine, phentolamine, concanavalin A (Con A), and filipin were purchased from Sigma Chemical (Poole, Dorset, UK). Prazosin HCl was supplied by Sigma/RBI (Natick, MA), and [^{3}H]prazosin (0.2 nM; specific activity 76 Ci/mmol) was from Amersham Biosciences Inc. (Piscataway, NJ). Hoechst 33342, BODIPY-FL-labeled prazosin (QAPB), BODIPY-R 558/568-labeled prazosin (RQAPB), Lysotracker Red DND-99, and transferrin (Tfn)-Alexa Fluor^{546} were purchased from Molecular Probes (Eugene, OR). All optical fluorescence filters were purchased from Chroma Technology Corp. (Rockingham, VT).

Stock solutions for each chemical were prepared in distilled water or dimethyl sulfoxide and subsequently aliquoted and stored at −20°C. These stock solutions were diluted to working concentrations in physiological salt solution on each experimental day.

Construction of Plasmids

Production and subcloning of α_{1a}-AR-EGFP2 involved polymerase chain reaction amplification of the human α_{1a}-AR sequence using the amino-terminal primer 5′-AAA AGG TAC CAT GGT GTT TCT CTC GGG AAA TGC TTC-3′ to introduce a KpnI restriction sequence upstream of the coding sequence. Using the carboxy-terminal primer 5′-AAA AGG ATC CGA CTT CCT CCC CGT TCT CAC TGA GGG-3′, the receptor stop codon was removed, and a BamH1 restriction enzyme site was introduced downstream of the receptor coding sequence. The resulting polymerase chain reaction fragments were then ligated either into the multiple cloning site of the pEGFP2 N2 vector (PerkinElmer Life and Analytical Sciences) or the expression vector pcDNA3 (Invitrogen, Carlsbad, CA) to form the EGFP2-tagged and non-EGFP2-labeled version of the human α_{1a}-AR, respectively. Each construct was fully sequenced before its expression and analysis. β-Arrestin-2-EGFP was obtained from Dr. C. Krasel (Department of Pharmacology, University of Würzburg, Germany).

Cell Culture and Transfection

R-1Fs stably expressing the bovine α_{1a}-AR were grown in DMEM supplemented with 5% (v/v) newborn calf serum, penicillin (100 IU/ml), streptomycin (100 μg/ml), and L-glutamine (1 mM) in a 95% air and 5% CO_2 atmosphere at 37°C. Selection was maintained by adding G418 (400 μg/ml) to the growth media.

HEK293T cells were maintained in DMEM supplemented with 0.292 g/l L-glutamine and 10% (v/v) newborn calf serum and incubated at 37°C with 5% CO_2. HEK293T cells were grown on glass coverslips to ~70% confluence before transient transfection with the appropriate human α_{1a}-AR plasmid using LipofectAMINE reagent (Invitrogen). After 4 h, cells were washed twice with Opti-MEM I and cultured in DMEM for 24 h. A total of 3 μg of pEGFP2 N2 vector or pCDNA3 containing the human α_{1a}-AR cDNA was used to transfect each coverslip. Mouse embryo fibroblasts (MEFs) derived from both wild-type and β-arrestin 1 plus β-arrestin 2 knockout animals have been described previously (Kohout et al., 2001) and were obtained from Dr. R. J. Lefkowitz (Duke University, Durham, NC). These were maintained in DMEM supplemented with 0.292 g/l L-glutamine and 10% (v/v) fetal calf serum at 37°C in a 5% CO_2 environment. Cells were grown to 60 to 80% confluence before transient transfection on sterile glass coverslips. Transfection (3 μg of cDNA) was carried out using the Amaxa nucleofector system (Cologne, Germany) according to the manufacturer's instructions using program T20.

Radioligand Binding

Competitive α_1-AR binding assays were performed as described previously (MacKenzie et al., 2000). In brief, R-1F homogenates (0.05 mg/ml) stably expressing the bovine α_{1a}-AR were incubated in triplicate with the nonselective α_1-AR antagonist [^{3}H]prazosin (0.2 nM) in the presence or absence of a range of increasing concentrations of competing ligands in a total volume of 0.5 ml of Tris-HCl assay buffer. Nonspecific binding was determined as radioligand binding in the presence of 10 μM phentolamine. All equilibrations were carried out for 30 min at 25°C, and bound ligand was separated from free ligand by rapid cold vacuum filtration over Whatman GF/C filters (Whatman, Maidstone, UK) using a Brandel cell harvester. Concentrations of displacing agent eliciting 50% displacement of [^{3}H]prazosin (IC_{50}) were interpolated with the use of nonlinear iterative

curve-fitting methodologies performed by Prism 4.02 (GraphPad Software Inc., San Diego, CA) and converted into pK_i values with the equation of Cheng and Prussoff (1973).

Fluorescence Experiments Undertaken in R-1Fs

Epifluorescence Imaging of QAPB Binding to Spontaneously Recycling Bovine α_{1a}-ARs. R-1Fs stably expressing the bovine α_{1a}-AR were grown on sterile coverslips 24 h before experimentation. Coverslips were mounted into a flow chamber, placed on to the microscope stage, and superfused (5 ml/min) with HEPES-buffered saline solution at room temperature. Cells were illuminated using an ultrahigh-point intensity 75-W xenon arc lamp (Optosource, Cairn Research, Faversham, Kent, UK). A Nikon Diaphot inverted microscope equipped with a 40× oil immersion Fluor objective lens (1.3 numerical aperture) and a monochromator (Optoscan) set at an excitation wavelength of 490 nm (band pass 7 nm) was used to determine the background autofluorescence. After acquiring the background autofluorescence, the cells were superfused with fresh saline supplemented with the fluorescent antagonist ligand QAPB (5 nM) until equilibrium binding of QAPB occurred. QAPB fluorescence emission was detected by a cooled digital charge-coupled device camera (Cool Snap-HQ; Photometrics, Tucson, AZ). MetaFluor imaging software (version 4.6.9; Universal Imaging Corporation, Downingtown, PA) was used for control of the monochromator and charge-coupled device camera and for processing of all the cell image data and movie animations.

Sequential QAPB images (2 × 2 binning) were collected at 5-s intervals to determine the total QAPB fluorescence intensity associated with each cell, and exposure to excitation light was 60 ms/image. QAPB binding to α_{1a}-ARs was time dependently reversed by washing with QAPB ligand-free saline solution, with or without 100 μM phentolamine (the latter was incorporated to prevent rebinding of dissociating ligand and therefore to approximate infinite dilution conditions).

Quantification of the Fraction of QAPB Ligand-Receptor Complexes That Are Intracellular versus Surface at Steady State. Receptor expression at the cell surface (i.e., cell membrane, clathrin-coated pits) was defined as the rapid, initial, diffuse QAPB fluorescence that occurs after ligand addition but before the fluorescent ligand-receptor-containing endocytic vesicles can be visually resolved. Subtraction of the cell surface fluorescence from the total fluorescence allowed us to determine the intracellular fluorescence, and the maximal intracellular fluorescence was normalized to the maximal total QAPB fluorescence measured at steady state.

The rate of development of QAPB-associated or -dissociated fluorescence was determined by fitting one-phase exponential association or dissociation equations (via nonlinear regression), to each data point (GraphPad Software Inc.). The reciprocal of the rate constant was used to determine $t_{1/2}$ values.

Reversal of QAPB Fluorescence Binding to α_{1a}-ARs by the Competitive α_1-Antagonist Ligand Phentolamine. Spontaneously recycling α_{1a}-ARs were pre-equilibrated with QAPB (5 nM) for 75 min at room temperature before an image was acquired to determine the total QAPB fluorescence intensity associated with each R-1F. Sequential QAPB images (2 × 2 binning, 60 ms/image) were collected at 15-s intervals for a further 15 min to determine that equilibrium binding of QAPB had taken place before superfusion of the cells with saline containing QAPB (5 nM) plus phentolamine (10 μM). R-1Fs were equilibrated with this solution until the ligands QAPB and phentolamine had reached their new steady-state receptor occupancies. The remaining QAPB-associated fluorescence was then time-dependently removed by exposing the cells to saline containing the same concentration of QAPB (5 nM) plus a higher concentration of phentolamine (100 μM).

Using the editing capability of MetaFluor, QAPB intensity values derived from groups of R-1Fs were obtained by manually delimiting the profile of the cells and averaging the signals within the delimited region of interest for each time-lapse image captured. These averaged QAPB intensity values were exported into Prism 4.02 (GraphPad Software Inc.) and plotted over time.

Histogram Intensity Plots. Binned pixel intensities (8-bit image of 256 intensities divided into nine intensity bins) of fluorescence histograms representative of the localization of QAPB-labeled α_{1a}-ARs (over time) were computed using the histogram plot profile tool of MetaMorph 6.2.6 software (Universal Imaging Corporation). Background-subtracted image acquired at 0 s was determined as cell autofluorescence, and the pixel intensity of membrane QAPB fluorescence was calculated as the diffuse fluorescence that was observed after 2-min exposure to the ligand. To remove contributions of the plasma membrane signal into the intracellular QAPB signal, the diffuse fluorescence observed at 2 min was subtracted from all subsequently acquired images.

Binned integral counts acquired at various time intervals after addition or removal of the QAPB ligand were measured and expressed as intensity integral counts. QAPB binding to α_{1a}-ARs was detected as a shift to the right of the autofluorescence plot (at 0 s), and the quantified histogram data were used for comparison of intensity in various structures within the image data. Loss of QAPB from cycling α_{1a}-ARs was detected as a progressive shift to the left of the fluorescence intensity measured at equilibrium.

Image Analysis Colocalization

For the analysis of RQAPB-labeled bovine α_{1a}-ARs with β-arrestin-2-EGFP2, a region of no fluorescence adjacent to the cell was used to determine the average background level of fluorescence in the EGFP2 and RQAPB channels. The background amount was then subtracted from each pixel in each channel. Using the editing capability of MetaFluor, QAPB intensity values derived from groups of R-1Fs were obtained by manually delimiting the profile of the cells. Using the editing function a region of interest was manually drawn in the EGFP2 channel image, then selected and transferred to the matched image acquired in the RQAPB channel. Correlation coefficients were evaluated by comparing the amounts of fluorescence measured in each matched pixel of the two different channels using the MetaMorph "correlation plot" application.

Blockade and Reversal of QAPB Fluorescence Binding to Recycling α_{1a}-ARs by Concanavalin A and Hyperosmotic Sucrose, but Not Filipin. To study the role of clathrin-coated vesicles and caveolae in α_{1a}-AR endocytosis, the effects of hyperosmotic sucrose, Con A, and filipin on QAPB binding to recycling α_{1a}-ARs were assessed as follows. R-1Fs were superfused with saline, and a background autofluorescence image was acquired. R-1Fs were then pre-equilibrated with QAPB (5 nM) for 90 min at room temperature, which was sufficient time for QAPB binding to α_{1a}-ARs to reach equilibrium. An image was then acquired to determine the total QAPB fluorescence intensity. QAPB fluorescence was then completely removed by superfusing the cells with ligand-free saline for 90 min, and a background autofluorescence image was acquired. The R-1Fs were re-exposed to control saline or saline supplemented with Con A (0.25 mg/ml), hyperosmotic sucrose (0.45 M), or filipin (5 μg/ml) for 30 min before re-exposing the cells to QAPB (5 nM) in the continued presence of each individual inhibitor. QAPB intensity values were quantified by manually delimiting the profile of the fibroblast cells and averaging the QAPB fluorescence intensity within the delimited region of interest. All values of QAPB fluorescence intensity were corrected for background autofluorescence and the equilibrium QAPB intensity on this first exposure was normalized to 1. On a second exposure to QAPB, with or without test drugs, fluorescence intensity was measured at 30, 60, and 90 min and normalized to the "first exposure" value. Normalized data from each experimental group were pooled and are presented as mean ± S.E.M. Statistical significance between the means was evaluated using a Student's paired t test.

Multiple Fluorescent Labeling of Recycling and Late Endocytic Vesicles. R-1Fs seeded on to coverslips were rinsed with PBS and then exposed at room temperature to PBS containing either

10 nM QAPB and the recycling endosomal marker Tfn-Alexa Fluor^{546} (20 μg/ml) or the late endosomal/lysomal marker Lysotracker Red DND-99 (150 nM). Cells were pulse-labeled with Tfn-Alexa Fluor^{546} (37°C) or Lysotracker Red (room temperature) plus QAPB (10 nM) for 20 and 70 min, respectively. At the end of each pulse-labeling period, cells were rinsed with PBS supplemented only with QAPB (10 nM) and then bathed in this solution for a further 15 min. Approximately 10 min before image acquisition, cells were exposed to PBS containing 10 nM QAPB plus the nuclear DNA-binding dye Hoechst 33342 (10 μg/ml; 10-min incubation at room temperature) to stain cell nuclei. Each coverslip was then washed and bathed in QAPB containing PBS before being imaged. The dyes Hoechst 33342, QAPB, Tfn-Alexa Fluor^{546}, and Lysotracker Red were sequentially excited using the appropriate dichroics/filters to prevent bleed through, and the resultant images were overlaid using MetaMorph software (version 6.2.6).

3D visualization of the colocalization of QAPB ligand-bovine α_{1a}-AR complexes with Tfn-Alexa Fluor^{546} or Lysotracker Red was achieved by using a Nikon TE2000-E inverted microscope equipped with a *z*-axis linear encoded stepper motor. Each dye was sequentially excited, and a z-series of images were acquired at 0.22-μm steps to produce individual z-stacks. The z-stack images were then merged and deconvoluted using an iterative and constrained algorithm (Autodeblur software, version 9.3.4; Autoquant Imaging, Watervliet, NY). Triplicate 3D (x-y, x-z, and y-z) maximum projection views were constructed using Autovisualize software (Autoquant Imaging).

Fluorescence Experiments Undertaken in Wild-Type and β-Arrestin Double Knockout Mouse Embryo Fibroblasts. Twenty-four hours after transfection with the α_{1a}-AR-EGFP2 fusion protein, cells were observed under oil immersion, and fluorescence images were acquired at different time intervals in the absence or presence of the RQAPB ligand. During image acquisition, cells were maintained by superfusing them with HEPES-buffered saline solution. EGFP2 and RQAPB were excited using the appropriate wavelength (490 nm for EGFP and 545 nm for RQAPB) and emitter (BP505-545 for EGFP and BP585-625 for RQAPB (Chroma Technology Corp.). 3D imaging was undertaken as described previously, and 3D volumetric measurements of the proportion of surface EGFP2-tagged receptors binding RQAPB (relative to the total EGFP2-tagged α_{1a}-ARs) was determined using Autodeblur software, version 9.3.4 (Autoquant Imaging).

Fluorescence Experiments Undertaken in HEK293T Cells

Dual Hoechst and QAPB Epifluorescence Imaging. HEK293T cells transiently transfected with the non-EGFP2-tagged version of the human α_{1a}-AR were rinsed several times in PBS and then exposed to QAPB (10 nM) for 70 min at room temperature. Cell nuclei were stained before visualization. QAPB and Hoechst were sequentially excited and detected as detailed previously. Sequential images (no binning) were collected at 15-s intervals.

Dual EGFP2 and RQAPB Confocal Imaging. Cells were plated onto glass coverslips (22 mm), and after a 24-h growth period, they were transiently transfected with the EGFP2-tagged version of the human α_{1a}-AR. Transfected cells were cultured overnight, and 24 h later, growth medium was removed and replaced with fresh PBS. Transfected cells were then pre-equilibrated with fresh PBS containing 10 nM RQAPB (a red fluorescent variant of the antagonist ligand QAPB) for 75 min. The RQAPB-treated cells were mounted onto an imaging chamber, and a Zeiss 510 PASCAL laser scanning confocal inverted microscope equipped with a 63× oil immersion Plan Fluor Apochromat objective lens (1.4 numerical aperture) was used to visualize each fluorescent probe. Using the appropriate laser lines (i.e., 488 nm for EGFP2 and 543 nm for RQAPB) and emission filters (i.e., BP505-530 for EGFP2 and LP570 for RQAPB), sequential images were acquired to determine the total EGFP2 and RQAPB fluorescence emission intensity associated with each transfected cell. Overlay images were created as outlined previously.

Solutions. HEPES-buffered saline solution contained 130 mM NaCl, 5 mM KCl, 1 mM $CaCl_2$, 1 mM $MgCl_2$, 20 mM HEPES, and 10 mM D-glucose, pH adjusted to 7.4 using NaOH. Tris-HCl assay buffer composition was 150 mM NaCl, 50 mM Tris-HCl, 10 mM $MgCl_2$, and 5 mM EDTA, pH 7.4.

Results

Affinities of Compounds Measured by [^{3}H]Prazosin Competition Binding

Binding affinity estimates for the ligands used in this study were determined in R-1Fs stably expressing the bovine α_{1a}-AR to set the quantitative context for visualization of ligand-ligand competition. Competition curves in membrane preparations between [^{3}H]prazosin and both prazosin and its fluorescent analog QAPB were monophasic and exhibited Hill coefficients that were close to unity (Fig. 1). Prazosin and QAPB displayed subnanomolar affinity for the receptor. The pK_i value of phentolamine was 8.5, and this ligand was used at high concentration (10 μM) to determine nonspecific binding.

Direct Visualization of the Fluorescent Ligand-α_{1a}-AR Complex

Does Fluorescent Ligand Binding Coincide with Receptors? Nontransfected HEK293T cells showed no fluorescence on exposure to QAPB (10 nM) for 75 min (Fig. 2A, i and ii). Similar exposure of cells transfected with the α_{1a}-AR produced fluorescence predominantly in intracellular punctate vesicles, with a lower level reflecting cell surface localization (Fig. 2B). This is consistent with the concept that unbound QAPB does not fluoresce and that binding to the α_{1a}-AR occurs with high affinity. In cells transfected with the α_{1a}-AR-EGFP2 fusion protein, EGFP2 autofluorescence had a similar distribution (Fig. 2C, i) to QAPB in α_{1a}-AR (no EGFP2) cells (compare with Fig. 2B). In the α_{1a}-AR-EGFP2-expressing cells, exposure to the red version of QAPB produced red fluorescence (Fig. 2C, ii) that colocalized with the

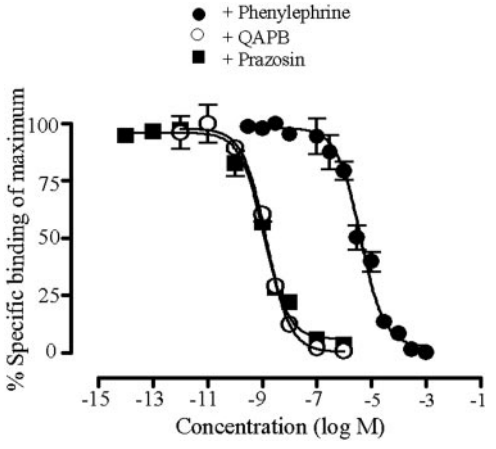

Fig. 1. Affinities of compounds measured by [^{3}H]prazosin competition binding in R-1Fs stably expressing α_{1a}-AR. Competition between [^{3}H]prazosin (0.2 nM) and increasing concentrations of phenylephrine (circles; n = 4), QAPB (open circles; n = 6), and prazosin (squares; n = 4) for binding to membranes prepared from R-1Fs expressing the bovine α_{1a}-AR. Assay points were determined in triplicate, and nonspecific binding was determined in the presence of phentolamine (10 μM). The pK_i and n_H values for these compounds are listed in Table 2.

green fluorescence of EGFP2 (Fig. 2C, iii). This indicates that 1) on incubation with live cells, QAPB binds to, and thus indicates the location of, all the α_{1a}-AR population; 2) the ligand gains access to all compartments containing the EGFP2-labeled α_{1a}-AR; 3) the receptor has affinity for the ligand at all of these sites (because unbound ligand does not fluoresce); 4) the EGFP2 tag does not alter receptor distribution or the movement of the organelles that they inhabit; and 5) QAPB did not change the cellular disposition of EGFP2-tagged receptors, unlike agonists, which can cause a visible shift toward internalization. The similarity of the distribution of EGFP2 and QAPB also confirmed that the relative lack of cell surface QAPB binding is an accurate reflection of the proportion of the receptor population at the plasma membrane rather than a technical artifact. As in HEK293T cells, QAPB labeling of the α_{1a}-AR stably expressed in R-1F cells confirms the intracellular localization of the ligand-receptor complex in a second cell type. Data are presented as a 3D reconstruction [Fig. 2D, x-y view (i), x-z view (ii), and y-z view (iii); cell nuclei shown in blue and green punctate spots represent QAPB binding].

Transiently transfected HEK293T cells were suitable for demonstrating features of cell distribution and colocalization, but because they had variable expression of the transfected receptors, they were less suitable for quantitative analysis of fluorescence ligand binding than stably transfected fibroblast lines.

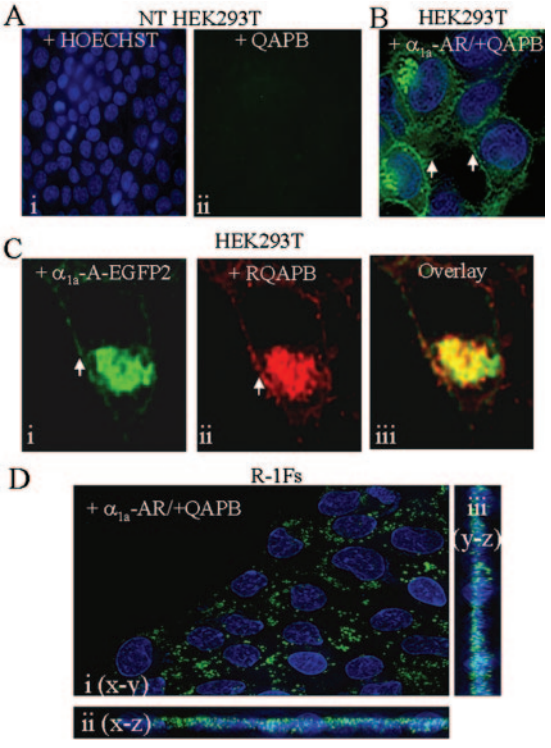

Fig. 2. Direct visualization of the fluorescent ligand-α_{1a}-AR complex and colocalization of the fluorescent ligand with human α_{1a}-AR-EGFP2 in HEK293T cells. A, Hoechst (blue)-stained nuclei and the level of QAPB (10 nM) fluorescence detected from the same field in nontransfected HEK293T cells is shown in image i and ii, respectively. B, human α_{1a}-AR was expressed transiently in HEK293T cells, and its distribution is visualized after 75-min exposure to 10 nM QAPB (green in overlay image of B). C, human α_{1a}-AR-EGFP2 was expressed transiently in HEK293T cells. Image i shows the distribution of EGFP2, and image ii shows the localization of RQAPB (10 nM) after 75-min exposure to the fluorescent antagonist ligand. Colocalization of the EGFP2 fusion protein and RQAPB is represented by yellow/orange in overlay image iii of C. D, 3D overlay maximum projection view of intracellular fluorescent α_{1a}-AR/QAPB ligand sites (green punctate vesicles) and Hoechst-stained nuclei (blue color) in R-1Fs is shown in images i–iii: x-y view (i), x-z view (ii), and y-z view (iii).

Time Course of Formation, Spatial Pattern, and Continuous Movement of Ligand-α_{1a}-AR Complexes. The equilibrated cells discussed above had indicated that QAPB gains access to all α_{1a}-AR in live cells. The time course of the appearance (and disappearance) of fluorescence allowed analysis of the processes involved. Time-lapse epifluorescence images over 75 min were constructed in R-1F cells stably transfected with wild-type receptor and using QAPB at a concentration (5 nM) near its equilibrium constant (Fig. 3). Events were most easily seen and could be readily plotted

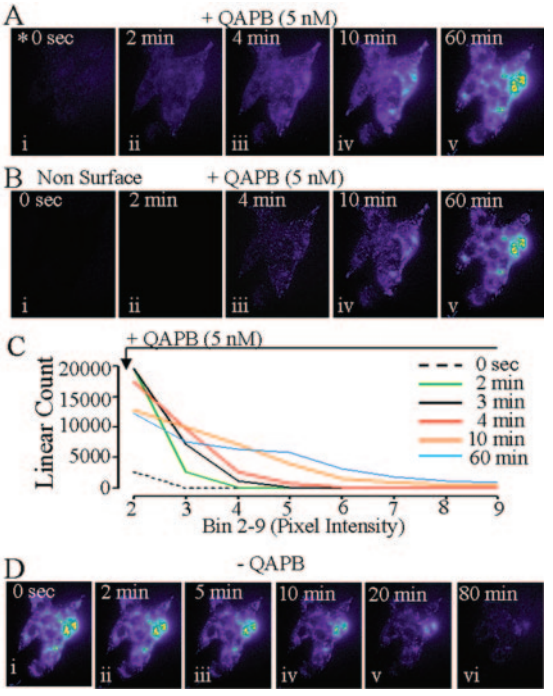

Fig. 3. Separation of α_{1a}-ARs in intracellular pools and at the cell surface and comparison of the changes in the distribution of fluorescent QAPB intensity during equilibration binding of QAPB and during loss of QAPB from recycling α_{1a}-ARs stably expressed in R-1F cells. A, time-lapse images presented show the development of QAPB (5 nM), fluorescence to steady state. Asterisk superimposed on image i of A represents the link to supplemental QuickTime Movie 1 (prepared from assembled time-lapse images of image i recorded at 5-s intervals), which can be viewed at http://molpharm.aspetjournals.org. Movie 1 revealed that some of the QAPB-labeled receptors displayed short-range bidirectional motion, whereas others were inert or moved vast distances. Image i represents the cell autofluorescence at 0 time (i.e., before the addition of QAPB. Image ii shows surface QAPB fluorescence (at 2 min). Image iii represents the distribution of surface and intracellular receptor QAPB fluorescence after 4-min exposure to the QAPB ligand. The distribution of surface and intracellular QAPB fluorescence at steady state is shown in image v. B, time-lapse images presented in B show a more sharpened view of the mobile intracellular organelles images when surface QAPB fluorescence binding at 2 min (Fig. 3A, ii) is subtracted from the time-series images presented in A. C, fluorescent intensity histogram of QAPB fluorescence distribution over time (bins 2–9 shown). Histogram shows the distribution pattern continually changes as QAPB equilibrates with recycling α_{1a}-ARs. Bin 1 (not shown) contains all the black pixels and background noise except a very small number that are shown in bin 2; at time 0, no other bin contains any pixels. Equilibration of QAPB with cycling α_{1a}-ARs was detected as a progressive shift to the right, indicating the gradual appearance of steadily brighter pixels until equilibrium is reached. D, loss of QAPB fluorescence over a 80-min wash period is shown in images i–vi.

by taking a two-dimensional view that keeps the fluorescence from the whole cell thickness in the focal plane.

Within 1 to 2 min, the cells were rapidly "covered" with ligand, as shown by low level diffuse fluorescence corresponding to binding to receptors on, or in proximity to, the cell membrane (Fig. 3A, ii). Slightly later, noticeable within 3 to 4 min of ligand application, higher intensity fluorescent signals occurred in punctate intracellular vesicles that were scattered throughout the cell cytoplasm (Fig. 3A, iii). Very soon after this (5–10 min), higher intensity fluorescent signals started to occur in larger punctate structures near the nucleus (Fig. 3A, iv), and their intensity increased steadily to equilibrium at 55 to 60 min (Fig. 3A, v). The pattern of fluorescence therefore evolves from a small particulate distribution toward larger structures with time. Asterisk superimposed on image i of Fig. 3A represents the link to supplemental QuickTime Movie 1 (created from assembled sequential time-lapse images of image i acquired at 5-s intervals).

Video sequence of Movie 1 revealed that some of the fluorescent objects displayed short-range bidirectional motion, whereas others were inert or moved vast distances across the body of the R-1F. Thus, the fluorescent organelles containing α_{1a}-ARs moved continuously, and this occurs in the absence of agonist stimulation.

This visual interpretation was confirmed quantitatively by binning the pixels according to their intensity (Fig. 3C) and then displaying the contents of each bin as a time course (Fig. 4A). In this way, the binding to receptors over the whole cell surface can be distinguished from binding to the punctate intracellular structures, which represent a smaller fraction of the image but are brighter. The lowest intensity bin (bin 1), which contains the black pixels and the background fluorescence, is omitted from the graphs. Bin 2 is the lowest intensity bin that shows specific fluorescence. This shows the rapid acquisition of the binding signal over the whole cell surface. It reached a peak at between 2 and 3 min, and at this time, there were no high-intensity signals because it was too early for the ligand to have reached the intracellular structures. However, after 3 min the higher intensity bins started to increase in sequence as the punctate intracellular structures occurred. A consequence of this was that the number of pixels in bin 2 decreased as the punctate structures took over their pixels. The time course of the increase in the number of pixels in the highest intensity bins indicates the slower acquisition of binding by the intracellular structures until ligand binding reached a steady state (at 40–60 min; Figs. 3A, image v; and 4A). Note that the total number of pixels in the "brighter bins" (bins 3–8) remained constant after 10 min, but the number in the brightest bins (bins 5–8) increased at the expense of the intermediate bins (bins 3 and 4); i.e., all the intracellular structures were fully revealed at 10 min, but they did not become saturated until 60 min.

Separation of α_{1a}-ARs in Intracellular Pools and at the Cell Surface in R-1Fs

Receptor expression on the cell surface can be estimated from the rapid, initial, diffuse binding that occurs after addition of ligand but before the intracellular organelles can be visually resolved. This occurred within 2 min (Fig. 3A, ii), indicating a rapid association rate for the ligand- and surface-located receptors. The sum of the cellular fluorescence at this point in time thus represents the total of the cell surface receptors. When equilibrium occurs, in a 2D image that visualizes everything in the cell, the image of the intracellular binding is superimposed upon this surface image. Subtraction of this image from the equilibrium image thus leaves the image of the intracellular binding (Fig. 3B). Because the surface image is constant, this subtraction can be applied to a time series of images to leave a much enhanced view of the mobile intracellular organelles (Fig. 3B) and proved a remarkably effective way of separating the images of the surface and intracellular ligand-receptor complex.

This information could then be used quantitatively to assess relative numbers of receptors on the surface and inside cells. Because the fluorescence at equilibrium represents the total receptor population, the proportion of receptors on the surface can be calculated from the ratio of binding at 2 min and at equilibrium, giving a surface population of 30% and intracellular of 70%. When the surface binding was subtracted from the binding at each time point a graph of the rate of binding detected in intracellular sites could be constructed (Fig. 4C; compare solid black line with broken line trace). From this graph, a rate constant for the appearance of intracellular binding could be estimated. The resulting $t_{1/2}$ of 12.4 min did not differ significantly from the equivalent value calculated from the total fluorescence [i.e., 12.5 min (2)].

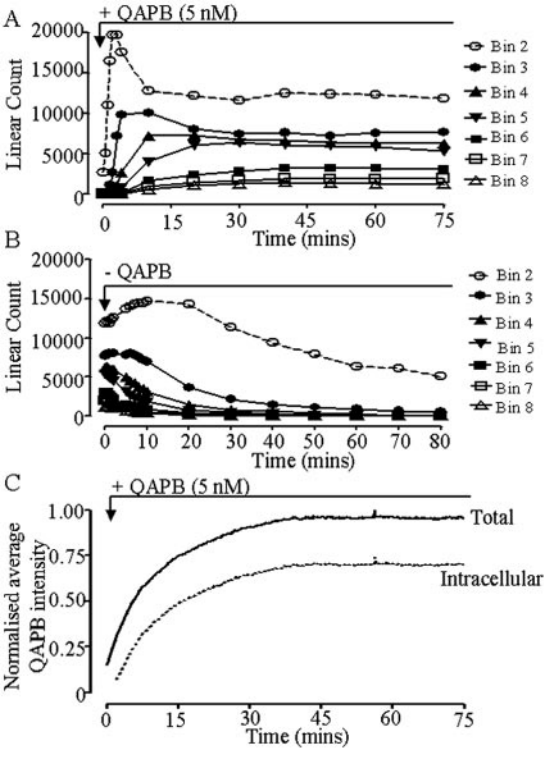

Fig. 4. Time course of the distribution of fluorescent QAPB intensity measured at steady state and during loss of QAPB from cycling α_{1a}-ARs in R-1Fs. A, fluorescent intensity time-course plot of onset of QAPB fluorescence binding over time (bins 2–8 shown, data reanalyzed from Fig. 3C). B, washout: the time-course plot during loss of QAPB from recycling receptors (bins 2–8 shown). C, development of total fluorescence (over time) associated with the binding of the QAPB ligand to α_{1a}-ARs to a steady state within 55 min. Black solid line corresponds to the total (surface and intracellular) QAPB fluorescence, whereas the broken black line represents the intracellular component after subtracting the surface binding represented by the fluorescence at 2 min (see image subtraction protocol outlined under *Materials and Methods*).

Reversal of Binding by Washing or the Competitive Antagonist Phentolamine

Washout. The binding of QAPB was reversible when the ligand was withdrawn from the superfusate (Figs. 3D and 5B). Viewing the time lapse or movie showed a steady fade of all parts of the image, but it was less easy to analyze visually than the "on" phase. Quantitative analysis showed essentially a reversal of the histogram intensity pattern compared with the on phase (a progressive shift toward lower intensity bins) (Fig. 4B). However, in contrast to the fast initial increase in low-intensity pixels in the on phase binding, the initial event was a slow but steady fall in the number of pixels across the high-intensity bins, suggesting that outgoing receptor-ligand complexes were replaced by vacant receptors (there is a corresponding increase in the number of low-intensity pixels in bin 2 as the punctate structures disappear). Although this is not dramatic on the histogram plot, because these pixels are of high intensity, the fall in overall fluorescence was substantial and rapid (Fig. 5B). The overall pattern was therefore of loss from the inside, with low-intensity surface binding last to disappear, as would be expected if ligand-receptor complexes steadily returned to the surface.

Phentolamine. Although washing with saline produced a rapid fall in QAPB fluorescence, the $t_{1/2}$ for the disappearance of fluorescence, 22.0 min (Table 1 was slower than for its appearance. This could be accounted for by reassociation of ligand because washing in the presence of an excess of phentolamine (100 μM; $n = 3$) increased the rate of loss of QAPB fluorescence by a factor of 2; $t_{1/2} = 10.7$ min (Table 1; Fig. 5B, pooled data points, dark gray line). Thus, the true rates of uptake and loss are very similar, at 12.5 and 10.7 min, respectively.

Phentolamine was able to displace fluorescent ligand even in the continued presence of QAPB (5 nM) in the saline. This was concentration-dependent (Fig. 5): 10 μM phentolamine was not fully effective (Fig. 5A, iii) but 100 μM was (Fig. 5A, iv, and B), thus establishing that all detectable binding was specific and that the fluorescent receptor-ligand complexes were susceptible to competitive ligands. Displacement in the continued presence of QAPB by phentolamine (100 μM) was slower than washing with or without phentolamine (Table 1; Fig. 5B, light gray line, $t_{1/2} = 25.6$ min; $n = 4$), as expected if some bound ligand continued to be internalized before equilibration with phentolamine had been attained.

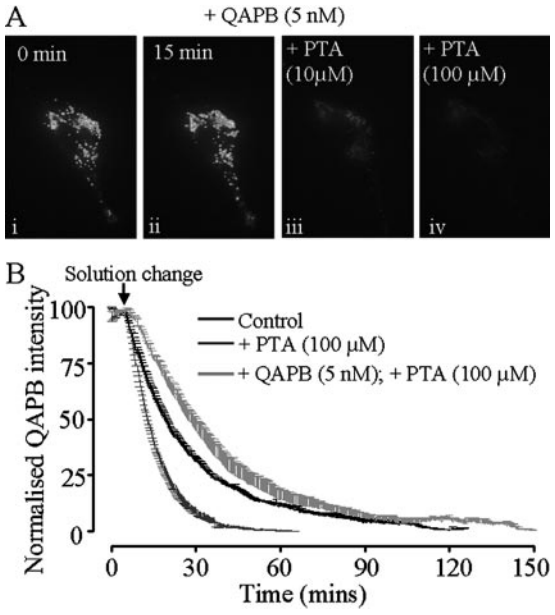

Fig. 5. Recycling α_{1a}-AR-QAPB ligand complexes are displaced by the competitive α_1-antagonist ligand phentolamine in R-1Fs stably expressing α_{1a}-AR. A, images i and ii show equilibrium binding of QAPB (5 nM) to recycling bovine α_{1a}-AR over 15 min (cell exposed to QAPB for 90 min in total). The images are nonidentical because the endosomes are mobile, but total fluorescence is constant. Phentolamine (iii; 10 μM, 240 min) almost abolishes fluorescence; phentolamine 100 μM (iv; a further 120 min) abolishes fluorescence. B, time course of loss of QAPB (5 nM) for 75-min fluorescence caused by wash, phentolamine or both; pooled data, mean ± S.E.M. Black trace illustrates the rate of loss on washing with QAPB-free saline ($n = 3$). Dark gray line shows a faster rate of loss in QAPB-free saline with phentolamine (100 μM; $n = 3$). Phentolamine (100 μM) given in the continued presence of QAPB (5 nM) produced complete displacement but took longer than when QAPB was removed (light gray trace; $n = 4$).

Estimation of Receptor Cycling Time and Residence at Cell Surface

If the receptor population is spontaneously cycling, the average time at the surface should be the same proportion of the total cycling time. The cycling time cannot be calculated accurately from these data, but its limits can. Because half-saturation is achieved in 12.5 min (Table 1), it is a reasonable working assumption that one inward leg of the cycle must occur within this time even if all receptors carried a bound ligand molecule (and the equilibrium binding data suggest that there would be on the order of 90% saturation, provided that the receptors were located at the surface long enough to equilibrate). This is supported by the rate of loss of fluorescence when the ligand was withdrawn in an excess of competitor, which was very similar; $t_{1/2} = 10.7$ min (Table 1). Together, these data allow the estimate that a full cycle is less than 25 min. Therefore, the average residence at the cell surface should be less than 7.5 min (30% × 25 min).

Is Endocytosis Involved in Internalization of Ligand?

The hypothesis that the QAPB ligand is internalized in association with recycling receptors was validated by blocking clathrin-coated pit/vesicle formation endocytosis using either Con A or hypertonic sucrose (Fonseca et al., 1995). It was first shown, quantitatively, that QAPB binding was reversible and reproducible (Fig. 6, open columns). Con A (0.25 mg/ml) or hyperosmotic sucrose (0.45 M) significantly inhibit the binding of QAPB (Fig. 6, black and gray columns) to recycling α_{1a}-ARs. After 30-min exposure to Con A or sucrose, QAPB fluorescence was inhibited by 84 ± 6% ($p < 0.001$; $n = 5$) and 85 ± 3% ($p < 0.001$; $n = 5$), respectively. This inhibition was maintained over 90 min with only a small further accumulation of fluorescence (Fig. 6). Filipin (5 μg/ml), an inhibitor of caveolar endocytosis, had no effect at any time point (shown at 90 min in Fig. 6B, dotted black column).

Is β-Arrestin Necessary for the Internalization or Trafficking of α_{1a}-ARs?

This was tested in MEFs devoid of β-arrestin 1/2. The α_{1a}-AR-EGFP2 fusion protein was predominantly expressed inside these cells in a clumped and clustered vesicular arrangement (Fig. 7A, i and ii, green, white arrows) that presumably reflects the well appreciated limitation of many transiently transfected cells to effectively mature and deliver receptors to the cell surface.

The asterisk on image i in Fig. 7A represents the link to Movie 2 prepared from assembled images of image i recorded at 15-s intervals. The video sequence of Movie 2 indicated that the intracellular, clumped pool of α_{1a}-AR-EGFP2 was motionless, in contrast with observations in wild-type MEF cells (see below). Despite this, in both sets of MEF cells, some of the α_{1a}-AR-EGFP2 fusion protein was localized at the cell surface (Fig. 7A, i and ii, green, red arrows). In the β-arrestin 1/2-deficient cells, after 75-min exposure to RQAPB (10 nM), the intracellular α_{1a}-AR-EGFP2 had not bound the RQAPB ligand (Fig. 7B, overlay image iv, white arrows). RQAPB did bind on the cell surface, where it colocalized with EGFP2-labeled surface α_{1a}-ARs (Fig. 7B, iv, red arrow, yellow represents colocalization). Asterisk on top of overlay image iv of Fig. 7B represents the link to Movie 3 showing a 3D y-z view of this image. Movie 3 clearly indicates the RQAPB ligand-α_{1a}-AR-EGFP2 complex (yellow) only on the surface of the MEF cell. The volume of α_{1a}-AR-EGFP2- (surface plus intracellular) and RQAPB-labeled α_{1a}-AR-EGFP2 complex (surface only) was 1823 and 1232 μm^3, respectively. The volume of intracellular EGFP2-tagged α_{1a}-ARs not labeled with RQAPB was 590 μM^3 (i.e., 32% of the total available EGFP2-tagged receptors). The relative fraction of surface to intracellular α_{1a}-ARs (at steady state), was 68 and 32%, respectively. This indicates that RQAPB did not gain access to the intracellular pool of α_{1a}-ARs in β-arrestin-negative MEF cells, demonstrating further that the ligand is not able to diffuse efficiently across the cell surface. By contrast, in wild-type MEF cells that express β-arrestins, the α_{1a}-AR-EGFP2 recycled (movie not shown), and after pre-equilibration with RQAPB (10 nM) for 75 min, it was observed that the RQAPB ligand colocalized with both cell surface (red arrow) and intracellular (white arrow) EGFP2-tagged α_{1a}-ARs (Fig. 7C, overlay image iv, yellow represents colocalization). Asterisk on overlay image iv of Fig. 7C represents the link to Movie 4 showing a 3D y-z view of this image. The video sequence of Movie 4 clearly shows the RQAPB ligand-α_{1a}-AR-EGFP2 complex (yellow) inside and on the cell surface. As anticipated from the above-mentioned description, nontransfected wild-type MEFs displayed no RQAPB fluorescence after 75-min exposure (Fig. 7C, compare image i with ii and iii.). These studies also support the hypothesis that RQAPB has to bind to cell surface receptors before its internalization and entry into the cell.

Are α_{1a}-AR-and β-Arrestin Found Together?

To answer this, R-1F cells were used that expressed both β-arrestin 2-EGFP and the bovine α_{1a}-AR. This resulted in nonuniform cytoplasmic localization of β-arrestin 2-EGFP with more intense β-arrestin-2-related fluorescence expressed in punctate vesicles (Fig. 8A, i, green vesicles some shown by white arrows). In contrast to this pattern, introduction of β-arrestin 2-EGFP into otherwise nontransfected R-1Fs resulted in a uniform cytoplasmic distribution of the tagged β-arrestin 2 (data not shown). Asterisk overlaid on image i of Fig. 8A represents the link to Movie 5 prepared from reconstructed sequential time-lapse 2D images of image i recorded at 15-s intervals. Movie 5 revealed that the organelles containing β-arrestin 2-EGFP showed rapid movement around the cells similar to that found for organelles carrying α_{1a}-ARs (Movie 5; Fig. 8A, i). No significant change in the localization or movement of β-arrestin 2-EGFP2 occurred upon exposure (15 min) to the agonist phenylephrine (3 μM) (Fig. 8A, compare image ii with iii). The same was found for the antagonist/inverse agonists prazosin (3 μM), phentolamine (3 μM), and RQAPB (10 nM) (data not shown).

When α_{1a}-ARs were labeled with RQAPB (10 nM), it partly colocalized with β-arrestin 2-EGFP (Fig. 8B, iv; yellow/orange punctate vesicles, some illustrated by white arrows). The degree of colocalization was quantified by plotting the amount of background-subtracted green EGFP fluorescence from the pixels in a region of interest (Fig. 8C, red rectangle superimposed on image ii and iii), against the amount of background red fluorescence in the corresponding pixels of the matched region in the RQAPB image. Correlation coefficients were quantified that described the degree by which EGFP and RQAPB fluorescence at each pixel within the region varied from a perfect correlation of 1.00. Calculated correlation coefficient was 0.91, indicating that RQAPB-labeled bovine α_{1a}-ARs colocalized very efficiently with β-arrestin-2-EGFP. Together, these data demonstrate partial, spontaneous association of α_{1a}-AR with β-arrestin-2EGFP- and indicate that α_{1a}-AR recycling is a β-arrestin-dependent, ligand-independent process.

Which Endosomal Compartments Does the Ligand-α_{1a}-AR Complex Enter?

To visualize and determine the identity of the intracellular compartments where the QAPB-receptor complexes resided, we examined potential colocalization with fluorescent reagents that can selectively identify different subcellular compartments. Tfn-Alexa Fluor^{546}, a recycling endosome fluorescent marker for endocytosis via clathrin-coated pits (Anderson, 1998; Gagnon et al., 1998), was used to identify the recycling pathway. Merged images, presented in Fig. 9A,

TABLE 1

Association and dissociation rate constant estimates of the development and loss of QAPB fluorescence from cycling α_{1a}-ARs

K values are represented as the mean ± S.E.M.

Ligand	Total	Total $t_{1/2}$	Intracellular	Intracellular $t_{1/2}$
	min^{-1}	*min*	min^{-1}	*min*
Control				
Association	$0.0802 \pm 3.865 \times 10^{-4}$	12.47	$0.0807 \pm 3.587 \times 10^{-4}$	12.39
Dissociation	$0.0824 \pm 3.137 \times 10^{-4}$	12.14	$0.1040 \pm 1.9207 \times 10^{-4}$	9.61
Wash (−PTA)				
Dissociation	$0.046 \pm 2.51 \times 10^{-4}$	22.00		
Wash (+PTA)				
Dissociation	$0.094 \pm 3.41 \times 10^{-4}$	10.70		
Wash (+QAPB, +PTA)				
Dissociation	$0.039 \pm 2.04 \times 10^{-4}$	25.60		

PTA, phentolamine.

iii, show that after 40 min, fluorescence corresponding to α_{1a}-AR-QAPB ligand sites (Fig. 9A, i, green punctates) partially overlapped with the fluorescent recycling marker (Fig. 9C, iii, yellow perinuclear vesicles, some indicated by white arrows). Some of the receptor-QAPB ligand binding sites were spatially distinct from the recycling endosomal Tfn receptors (Fig. 9C, ii, red punctates). A 3D x-z view of bovine α_{1a}-AR-QAPB ligand complexes partially colocalizing with recycling compartments (yellow punctates, white arrows) is shown in image iv of Fig. 9A.

Lysotracker Red DND-99, a highly selective red fluorescent acidotrophic probe for labeling acidic organelles (Bucci et al., 2000), was used to identify acidic late endosomes. After 90 min, Lysotracker Red fluorescence had extensive overlap with the intracellular structures binding QAPB (Fig. 9B, iii, yellow punctates, some shown by white arrows, compare images i, ii, and iii in Fig. 9B), implying that α_{1a}-AR ligand complexes were trafficked to the late endosomal/lysomal network. The 3D x-z colocalization view of bovine α_{1a}-AR-QAPB ligand complexes fusing with late/lytic endosomes is shown in Fig. 9B, iv (yellow punctates, white arrows).

Discussion

Visualizing the receptor/ligand complex in real-time demonstrates that the α_{1a}-AR is spontaneously internalized by endocytosis when expressed in a range of cells, including R-1Fs. The receptor continuously recycles, spending a relatively small fraction of time at the cell surface. Most of the time, each receptor molecule is present in intracellular organelles that shuttle between the cell surface and perinuclear compartments, including early and late endosomes. Both receptor internalization and the formation and movement of the mobile intracellular organelles are dependent on β-arrestins but not on receptor activation.

TABLE 2
Radioligand binding affinity and Hill slope estimates
pK_i values (means ± S.E.M.) and n_H were evaluated for each test ligand. Values of n represent the number of individual experiments.

Ligand	pK_i	n_H	n
Prazosin	9.26 ± 1.33	0.91 ± 0.15	4
QAPB	9.14 ± 1.70	1.08 ± 0.11	6
Phenylephrine	5.70 ± 0.32	0.78 ± 0.10	4

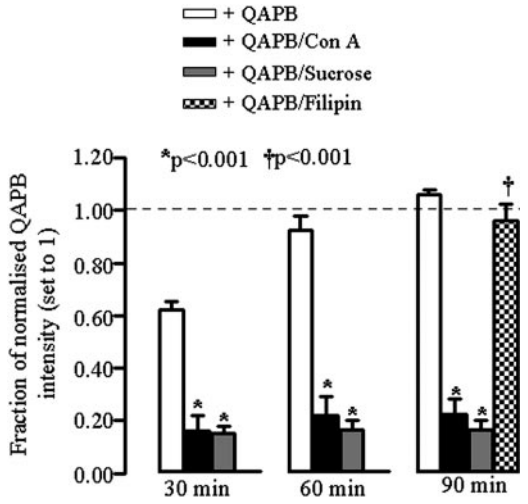

Fig. 6. Blockade of QAPB fluorescence binding to recycling α_{1a}-ARs by concanavalin A and hyperosmotic sucrose but not filipin in R-1Fs. R-1Fs stably expressing α_{1a}-ARs were preequilibrated with QAPB (5 nM) for 90 min at room temperature. Graph presented is pooled normalized data showing that preincubation of the R-1Fs with Con A (0.25 mg/ml) (black column; $n = 5$) or hyperosmotic sucrose (0.45 M) (gray column; $n = 5$) but not filipin (5 μg/ml) (dotted black column; $n = 3$, shown only at 90 min) significantly ($p < 0.001$) inhibits QAPB binding to α_{1a}-ARs. *, $p < 0.001$, Con A or sucrose data (30, 60, and 90 min) versus normalized QAPB fluorescence data (measured upon initial equilibrium binding of QAPB, value set to 1). †, $p < 0.001$, filipin versus Con A or sucrose data.

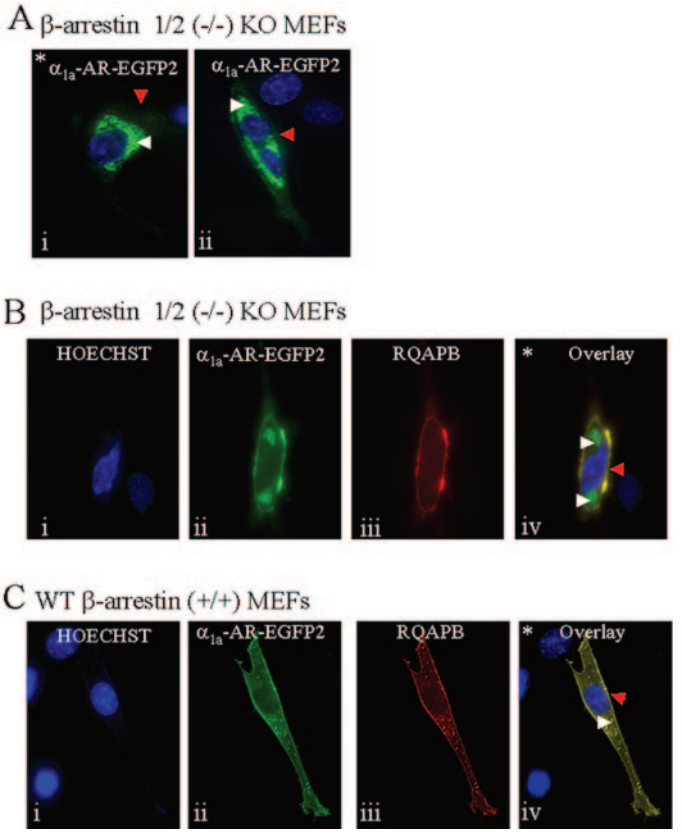

Fig. 7. Internalization of α_{1a}-AR-EGFP2 in MEF cells is β-arrestin-dependent. A, β-Arrestin 1/2-deficient MEF cells were transiently transfected with an α_{1a}-AR-EGFP2 fusion protein. Images i and ii show that the α_{1a}-AR-EGFP2 fusion protein was predominantly expressed inside the cell in a clustered vesicular arrangement (green, white arrows) with a lower level of expression localized on the membrane surface (light green, red arrows). Nuclei are shown in blue. Asterisk on image i of A represents the link to Movie 2 prepared from assembled time-lapse images of image i recorded at 15-s intervals. Movie 2 indicated that the intracellular, clumped pool of α_{1a}-AR-EGFP2 was motionless, in contrast with observations in wild-type MEF cells. B, blue, green, and red in images i to iii show the location of cell nuclei, α_{1a}-AR-EGFP2 fusion protein, and RQAPB (10 nM), respectively, in β-arrestin 1/2-deficient MEFs after preincubation with RQAPB for 75 min. Overlay image iv shows that although RQAPB (10 nM) can bind to cell surface α_{1a}-AR-EGFP2 (red arrow, yellow represents colocalization), it cannot access the intracellular pool (green, white arrows). Asterisk on top of overlay image iv of B represents the link to Movie 3 showing a 3D y-z animated view of this image. Movie 3 clearly shows the RQAPB ligand-α_{1a}-AR–EGFP2 complex (yellow) only on the surface of the MEF cell. C, wild-type, β-arrestin 1/2-expressing MEFs. Images i to iii are analogous to those in B. The cells show a more "normal" distribution of GFP-labeled receptors (i.e., with membrane and intracellular punctate distribution as in HEK293 and R-1F cells). Asterisk on overlay image iv of C represents the link to Movie 4 showing a 3D animated y-z view of this image. Movie 4 shows clearly that the RQAPB ligand internalized and colocalized with surface (red arrow) and intracellular (white arrow) α_{1a}-AR-EGFP2 (C, iv). Nontransfected wild-type MEFs (e.g., nucleus at bottom left with no associated GFP) display no RQAPB fluorescence, serving as another control.

Cycling is continuous and rapid, with complete turnover within 50 to 60 min. This has implications for understanding the "purpose" and properties of recycling and the dynamics of drugs acting at the receptors. The rate of agonist-induced internalization is not known in the case of α_{1a}-AR, but it is more resistant to desensitization than α_{1b}-AR (Vazquez-Prado et al., 2000). Agonist-induced internalization, as judged by disappearance of cell surface receptors, is undetectable for tagged α_{1a}-ARs in R-1Fs after 10 min (Price et al., 2002) and achieves small reductions even after 60 min of high concentrations of agonists (Stanasila et al., 2003; Morris et al., 2004). These net shifts of location may of course disguise an increase in recycling, with only the net shift in location being detected. Thus, constitutive recycling is the phenomenon more likely to occur in physiological conditions.

Agonist-induced recycling of α_1-AR has yet to be demonstrated at physiological concentrations of natural agonists or in native cells. When the α_{1a}-AR is localized in native cells such as smooth muscle or hepatocytes, it has consistently shown a predominant intracellular location coupled with a less dominant plasmalemmal location (Mackenzie et al., 1998, 2000; Hrometz et al., 1999; McGrath et al., 1999; Deighan et al., 2004; Miquel et al., 2005; for review, see Daly and McGrath, 2003). This could result from modulation by low levels of physiological agonist activation. Spontaneous α_{1a}-AR recycling may maintain an internal reserve pool of receptors that can sustain continuous agonist-induced signaling in the face of stimulation-induced attrition of the surface population, as suggested by Morris et al. (2004).

Our current advance is the ability to visualize and follow the receptor-ligand complex in real time. EGFP2-tagged receptors show total receptor localization but provide no information on movement within this population. Fluorescent antagonist ligands show the most recently labeled receptors that have internalized. Ligands access the interior of cells only if bound to endocytosing receptors because ligands enter only cells that possess both the receptor and β-arrestins.

The rate of appearance of intracellular fluorescence provides a time and concentration profile of the internalizing receptors from which rates of entry and of receptor recycling turnover can be estimated. This is analogous to the established use of antibodies to extracellular epitope tags for the study of internalization (Morris et al., 2004), but, additionally, can be followed in real time, and, in conjunction with

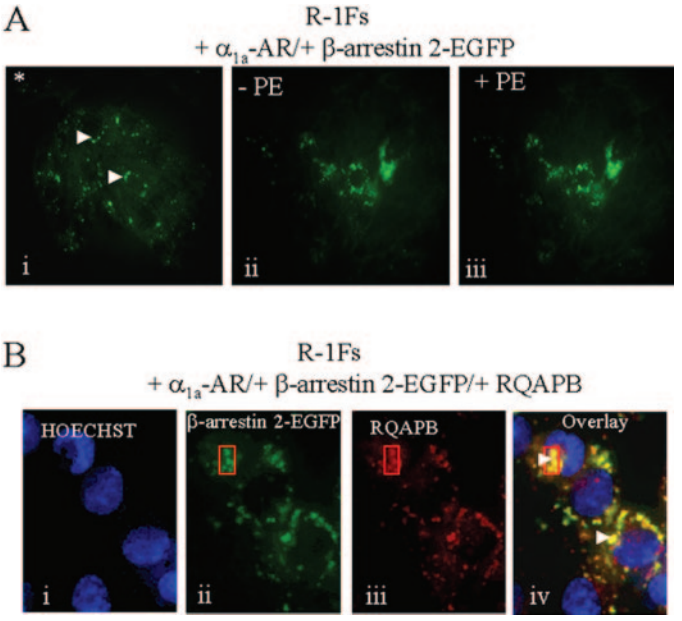

Fig. 8. Localization of β-arrestin 2-EGFP is agonist-independent, and it partially colocalizes with RQAPB-labeled α_{1a}-ARs. R-1Fs stably expressing bovine α_{1a}-ARs were transiently transfected with β-arrestin 2-EGFP. Twenty-four hours after transfection multifluorescence images were acquired from the same field of view. A, i, green vesicles represent the nonuniform, cytoplasmic localization of β-arrestin 2-EGFP with intense β-arrestin 2-related fluorescence expressed in punctate vesicles (some shown by white arrows). Asterisk overlaid on image i of A represents the link to Movie 5 prepared from reconstructed sequential time-lapse 2D-images of image i recorded at 15-s intervals. Movie 5 demonstrated that the organelles containing β-arrestin 2-EGFP showed rapid movement around the cells similar to that found for organelles carrying α_{1a}-ARs. Images ii to iii show that after 15-min exposure to the agonist phenylephrine (PE) (3 μM), no change in the localization of β-arrestin 2-EGFP2 was observed. B, colocalization of RQAPB-labeled bovine α_{1a}-ARs with β-arrestin 2-EGFP. i, blue represents cell nuclei. ii, green shows the localization of β-arrestin 2-EGFP2. iii, RQAPB pattern of fluorescence. iv, overlay image shows partial constitutive association (yellow/orange vesicles, some shown by white arrows) of bovine α_{1a}-AR-RQAPB ligand complexes with β-arrestin 2-EGFP. In the red rectangular region superimposed on images ii–iv, a pixel-by-pixel correlation of EGFP and RQAPB fluorescence was made (see text).

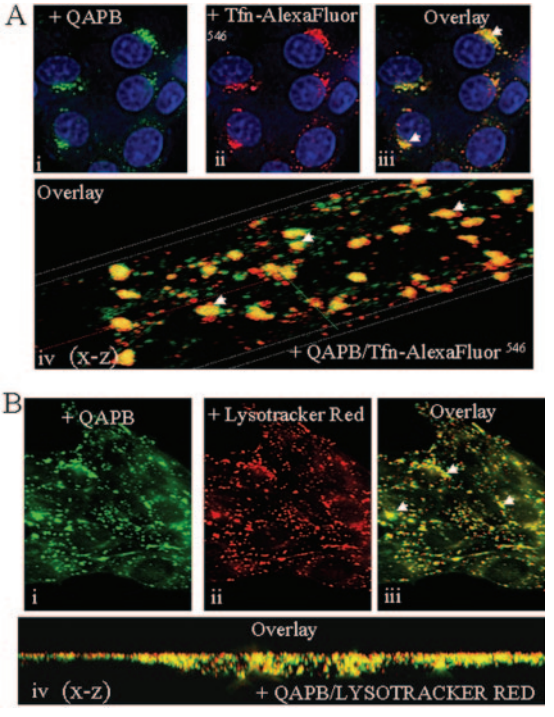

Fig. 9. Internalized QAPB ligand-α_{1a}-AR-complexes colocalize with recycling and late endosomal fluorescent markers in R-1Fs stably expressing α_{1a}-AR. A, colocalization with recycling compartments. i, green punctates represent QAPB (10 nM)-labeled α_{1a}-ARs, and blue shows nuclei stained with Hoechst. ii, recycling vesicles labeled with Tfn-Alexa Fluor^{546} are represented by the red punctate spots. iii, overlay image showing partial colocalization (yellow perinuclear vesicles) of bovine α_{1a}-AR-QAPB ligand complexes with the recycling endosomal marker. Iv, 3D x-z overlay maximum projection view, where yellow vesicles (some shown by white arrows) represent colocalization of QAPB-labeled bovine α_{1a}-ARs with the recycling marker. B, colocalization with late endosomes. i, green punctates represent QAPB (10 nM)-labeled α_{1a}-ARs. ii, late endosomes labeled with Lysotracker Red are represented by the red punctate vesicles. iii, red and green overlay image where yellow punctates represent colocalization of QAPB labeled bovine α_{1a}-AR with the late endosomal marker. iv, 3D x-z overlay maximum projection view of bovine α_{1a}-AR-QAPB ligand complexes colocalizing with the late endosomal marker (yellow vesicular structures, some represented by white arrows).

other vital dyes, can provide information on coincident dynamic events. The entire population recycles within 25 min, so the average residence time of the 30% at the cell surface is less than 7.5 min, even without stimulation.

The rapidity of these events has implications for receptor signaling and regulation. It cannot be assumed that internalized receptors are in a desensitized state that is incapable of signaling, although interaction with a β-arrestin will prevent concurrent interaction with G protein. An emerging literature indicates a distinct set of signaling functions for β-arrestins, particularly in the regulation of the kinetics and effectiveness of mitogen-activated protein kinase signaling cascades (Shenoy and Lefkowitz, 2003; Lefkowitz and Whalen, 2004). Although receptors are able to internalize with agonists bound, the low pH of recycling and other endosomes encourages dissociation, and it is likely that only high-affinity agonist ligands (e.g., peptides) remain bound throughout the cycle. Likewise, the paradigm of agonist-mediated internalization may require modification because agonists may simply accelerate spontaneous endocytosis rather than initiate it. A change in the balance of surface/intracellular receptors will occur only when the inward rate exceeds the rate of return to the surface, and this concept can be modeled mathematically (Koenig and Edwardson, 1997; Koenig, 2004).

Real-time visualization of movement of endosomal ligand-receptor complexes can allow the study of recycling in native cells, which was until now impractical because of the need for epitope tags. Receptors in mobile endosomes have been visualized previously only by using GFP-tagged G protein-coupled receptors (Koenig and Edwardson, 1997; Kallal and Benovic, 2002). Because an identical pattern of distribution and movement is found with the ligand or EGFP, their colocalization provides cross-validation of both techniques. Neither the EGFP2 tag nor the bound ligand slows endosomal movement or changes receptor distribution.

In cells devoid of β-arrestins, immobility of EGFP2-tagged receptor showed that β-arrestins are needed for the genesis of the mobile endosomes, a key part of the recycling system. Without them, receptors remained immobile in a fixed reticular endosomal compartment. Nevertheless, the proportion of receptors at the surface in β-arrestin-deficient MEF cells was similar to wild-type MEF cells, so β-arrestins are necessary for recycling, but recycling does not regulate partitioning of the receptor population.

Vesicles containing ligand-receptor complexes moved to and from the plasma membrane, indicating a ferrying function. This was visible for QAPB-labeled receptors in both R-1Fs and HEK293T cells and for EGFP2-labeled receptor in HEK293T cells. These movements are therefore an inherent property of the cells and not a phenomenon instigated by receptor occupation or cell type. The development with time of the intensity of these fluorescent structures when the cells were exposed to QAPB is akin to development of a photograph. Before uncovering the key role of endocytosis, it might have been assumed that ligand diffused into the cell, where it bound to internally located immobile receptors. Internalization of QAPB can now be understood in terms of endocytosis of a QAPB-receptor complex. In endocytosis, the basic units of transport are small structures, beyond the resolution of the microscope (e.g., caveoli or endocytic vesicles), that reversibly fuse with small visible structures to exchange a cargo of plasma proteins, including the ligand-receptor complex. These small fluorescent "transit" endosomes then move further into the cell and reversibly fuse with larger perinuclear endosomes, delivering ligand-receptor complexes.

Movements of transit vesicles and their transactions with the perinuclear complexes are made visible by the high concentrations of receptor-ligand complexes on their resolvable surfaces. The intensity per pixel shows receptor density to be 5 times higher than on the cell surface, indicating a high degree of physical marshaling and cargo selection. In all these intracellular transactions, the ligand and binding site are restricted to the internal face of endosomes, so that even if they dissociate, the ligand molecules will be restricted to the compartment and will be likely to reassociate. QAPB leaves the cell again on its removal from the extracellular environment, with a time course similar to its endocytic uptake, so it seems likely that it leaves the cell by the reverse process, bound to receptors recycling back to the cell surface.

Many α_1-AR antagonists are inverse agonists, including the quinazolyl-piperazine (e.g., prazosin, doxazosin, and alfuzosin) family to which QAPB belongs (García-Sáinz and Torres-Padilla, 1999; Price et al., 2002). However, the wild-type α_{1a}-AR receptor has low levels of constitutive activity (Rossier et al., 1999; Price et al., 2002). Furthermore, antagonists, including prazosin and QAPB, do not produce either a depression or a rise of resting intracellular Ca^{2+} concentration in these R-1F cells (Pediani et al., 2000), eliminating inverse agonism and partial agonism. In addition, Morris et al. (2004) showed that prazosin did not affect spontaneous endocytosis of the hemagglutinin-tagged α_{1a}-AR, and our data with phentolamine are consistent with competition and displacement of QAPB, rather than blockade of recycling.

Endocytosis was established as the entry mechanism for ligand-receptor complex using two independent agents (hyperosmotic sucrose and Con A) that block clathrin-mediated internalization (Daukas and Zigmond, 1985; Heuser and Anderson, 1989), and involvement of β-arrestins was confirmed by the absence of ligand uptake in β-arrestin-deficient MEF cells and by the partial colocalization of β-arrestin-2-GFP with the ligand/receptor. The generalization that interactions between receptor and β-arrestins require agonist-mediated phosphorylation of the receptor no longer holds. Such phosphorylation frequently increases the affinity of such interactions rather than defining them. For example, interactions between β-arrestins and the protease-activated receptor-1 are independent of receptor phosphorylation (Chen et al., 2004) as are such interactions with the BLT1 leukotriene B_4 receptor (Jala et al., 2005). However, the interactions of β-arrestins with components of the machinery of clathrin-mediated endocytosis are central to the delivery of β-arrestin/receptor complexes to clathrin-coated pits (Ferguson et al., 1996). Filipin, an inhibitor of caveolar endocytosis, had no major effect on uptake of QAPB. These results show that endocytosis via clathrin-coated vesicles is responsible for the ingress of QAPB.

The receptors initially enter in a similar manner as Tfn, and after a longer period penetrate endocytotic compartments beyond the limit of Tfn's ingress. Here, they are trafficked to more acidic vesicles: in the late endosomes, the receptors then go through a second stage of sorting and either are targeted to lysosomes for degradation or are slowly recycled back to the cell surface (Mellman, 1996; Resat et al.,

2003). Their dynamic equilibrium prevents easy distinction between early, late, and lysosome compartments, so we cannot estimate their relative proportions or the amount of receptor degradation. However, saline washing eliminated fluorescent ligand from cells, excluding accumulation in a compartment for long-term storage. A high proportion of the receptors were found in endocytic vesicles in both cells types used. This might be attributed to "overexpression" in these recombinant systems, but it is very similar to native systems such as smooth muscle cells from rat blood vessels and human prostate that express α_1-ARs (Mackenzie et al., 1998, 2000; McGrath et al., 1999; Deighan et al., 2004).

Spontaneous endocytosis responsible for internalization of the α_{1a}-AR and its antagonist ligand cargo is a new paradigm for uptake of antagonist drugs. It alters the potential mechanisms involved when whole cells are used in radioligand binding assay. Order of addition of drugs to cells becomes a potential source of variability, and time to equilibrium should be longer than if all binding were on the cell surface. When "membrane" preparations are used, many receptors will derive from intracellular membranes, and this may influence their properties, given the greater densities and the presence of different cofactors. Based on susceptibility to internalization, receptors are categorized into those that internalize/recycle constitutively or upon binding agonist (Milligan and Bond, 1997). However, receptors internalizing with antagonists attached do not fit this scheme. Agonist-independent G protein-coupled receptor internalization has been observed for the angiotensin AT_{1A} receptor and cholecystokinin receptors (Hein et al., 1997; Tarasova et al., 1997; Anborgh et al., 2000). For angiotensin AT_{1A} receptor, β-arrestin association with receptor, without agonist, is responsible for agonist-independent loss of cell surface receptor (Anborgh et al., 2000). The α_{1a}-AR can now be added to the "spontaneously recycling", β-arrestin-dependent category. How widely this applies among other G protein-coupled receptors remains to be seen. The cellular uptake of α-blockers at low concentrations also introduces a new concept into their mechanism of action in treating conditions such as benign prostatic hyperplasia. Intracellular concentration of drug at receptor-dense sites raises potential intracellular actions that require investigation and introduces new pharmacokinetic issues.

In conclusion, α_{1a}-AR recycle rapidly by agonist-independent, constitutive, β-arrestin-dependent processes. Receptors spend most of their time in endosomal recycling compartments and have a relatively short residence at the cell surface. Antagonists that bind to the receptive site are internalized with the receptor and transported through the recycling process, attaining saturation binding to intracellular receptors.

Acknowledgments

We thank Professor Gwyn Gould (Biochemistry and Molecular Biology, Institute of Biomedical and Life Sciences, University of Glasgow) for helpful discussions.

References

Anborgh PH, Seachrist JL, Dale LB, and Ferguson SSG (2000) Receptor/beta arrestin complex formation and the differential trafficking and resensitization of beta-2-adrenergic and angiotensin II type 1A receptors. *Mol Endocrinol* **14:**2040–2053.

Anderson RG (1998) The caveolae membrane system. *Annu Rev Biochem* **67:**199–225.

Bucci C, Thomsen P, Nicoziani P, McCarthy J, and van Deurs D (2000) Rab7: a key to lysosome biogenesis. *Mol Biol Cell* **11:**467–480.

Chen CH, Paing MM, and Trejo J (2004) Termination of protease-activated receptor-1 signaling by β-arrestins is independent of receptor phosphorylation. *J Biol Chem* **279:**10020–10031.

Cheng YC and Prusoff WH (1973) Relationship between the inhibitor constant (K_i) and the concentration of inhibitor which causes 50 percent inhibition of an enzymatic reaction. *Biochem Pharmacol Med* **22:**3099–3108.

Daly CJ and McGrath JC (2003) Fluorescent ligands, antibodies and proteins for the study of receptors. *Pharmacol Ther* **100:**101–118.

Daly CJ, Milligan CM, Milligan G, Mackenzie JF, and McGrath JC (1998) Cellular localization and pharmacological characterization of functioning α_1-adrenoceptors by fluorescent ligand binding and image analysis reveals identical binding properties of clustered and diffuse populations of receptors. *J Pharmacol Exp Ther* **286:**984–990.

Daukas G and Zigmond SH (1985) Inhibition of receptor-mediated but not fluid phase endocytosis in polymorphonuclear leucocytes. *J Cell Biology* **101:**1673–1679.

Deighan C, Woollhead AM, Colston JF, and McGrath JC (2004) Hepatocytes from α_{1B}-adrenoceptor knockout mice reveal compensatory adrenoceptor subtype substitution. *Br J Pharmacol.* **142:**1031–1037.

Ferguson SSG, Downey WE, Colapietro AM, Barak LS, Menard L, and Caron M (1996) Role of β-arrestin in mediating agonist-promoted G protein-coupled receptor internalization. *Science (Wash DC)* **271:**363–366.

Fonseca MI, Button DC, and Brown RD (1995) Agonist regulation of α_{1b}-ARs-adrenergic receptor subcellular distribution and function. *J Biol Chem* **270:**8902–8909.

Gagnon AW, Kallal L, and Benovic JL (1998) Role of clathrin-mediated endocytosis in agonist induced downregulation of the β_2-adrenergic receptor. *J Biol Chem* **273:**6976–6981.

García-Sáinz JA and Torres-Padilla ME (1999) Modulation of basal intracellular calcium by inverse agonists and phorbol myristate in rat-1 fibroblasts stably expressing α_{1d}-adrenoceptors. *FEBS Lett* **443:**277–281.

Hein, L. Meinel L, Pratt RE, Dzau VJ, and Kobilka BK (1997) Intracellular trafficking of angiotensin II and its AT_1 and AT_{1I} receptor: evidence for selective sorting of receptors and ligand. *Mol Endocrinol* **11:**1266–1277.

Heuser JE and Anderson RG (1989) Hypertonic media and Concanavalin A inhibit receptor-mediated endocytosis by blocking clathrin coated pit formation. *J Cell Biol* **108:**389–400.

Hrometz SL, Edelmann SE, McCune DF, Olges JR, Hadley RW, Perez DM, and Piascik MT (1999) Expression of multiple α_1-adrenoceptors on vascular smooth muscle: correlation with the regulation of contraction. *J Pharmacol Exp Ther* **290:**452–463.

Jala VR, Shao WH, and Haribabu B (2005) Phosphorylation independent beta-arrestin translocation and internalization of leukotriene B4 receptors. *J Biol Chem* **280:**4880–4887.

Kallal L and Benovic JL (2000) Using green fluorescent proteins to study G-protein-coupled receptor localisation and trafficking. *Trends Pharmacol Sci* **21:**175–180.

Kallal L and Benovic JL (2002) Fluorescent microscopy techniques for the study of G-protein-coupled receptor trafficking. *Methods Enzymol* **343:**492–506.

Koenig JA (2004) Assessment of receptor internalization and recycling. *Methods Mol Biol* **259:**249–273.

Koenig JA and Edwardson JM (1997) Endocytosis and recycling of G protein-coupled receptors. *Trends Pharmacol Sci* **18:**276–287.

Kohout TA, Lin F-T, Perry SJ, Conner DA, and Lefkowitz RJ (2001) β-Arrestin 1 and 2 differentially regulate heptahelical receptor signaling and trafficking, *Proc Natl Acad Sci USA* **98:**1601–1606.

Lefkowitz RJ and Whalen EJ (2004) beta-Arrestins: traffic cops of cell signaling. *Curr Opin Cell Biol* **16:**162–168.

Mackenzie JF, Daly CJ, Luo D, and McGrath JC (1998) Cellular localisation of alpha-1 adrenoceptors in native smooth muscle cells, in *Proceedings of the 5th Internet World Congress on Biomedical Sciences*; 1998 Dec 7–16; McMaster University, Hamilton, Ontario, Canada. Available from http://www.mcmaster.ca/inabis98/cvdisease/mackenzie089/index.html.

Mackenzie JF, Daly CJ, Pediani JD, and McGrath JC (2000) Quantitative imaging in live human cells reveals intracellular α1-adrenoceptor ligand-binding sites. *J Pharmacol Exp Ther* **294:**434–443.

McGrath JC, Arribas SM, and Daly CJ (1996) Fluorescent ligands for the study of receptors. *Trends Pharmacol Sci* **17:**393–399.

McGrath JC, Mackenzie JF, and Daly CJ (1999) Pharmacological implications of cellular localization of alpha1-adrenoceptors in native smooth muscle cells. *J Auton Pharmacol* **19:**303–310.

Mellman I (1996) Endocytosis and molecular sorting. *Annu Rev Cell Dev Biol* **12:**575–625.

Milligan G and Bond RA (1997) Inverse agonism and the regulation of receptor number. *Trends Pharmacol Sci* **18:**468–474.

Miquel MR, Segura V, Ali Z, D'Ocon MP, McGrath JC, and Daly CJ (2005) 3D image analysis of fluorescent drug binding. *Mol Imaging*, in press.

Morris DP, Price RR, Smith MP, Lei B, and Schwinn DA (2004) Cellular trafficking of human α_{1a}-adrenergic receptors is continuous and primarily agonist-independent. *Mol Pharmacol* **66:**843–854.

Pediani JD, MacKenzie JF, Heeley RP, Daly CJ, and McGrath JC (2000) Single-cell recombinant pharmacology: bovine α_{1a}-adrenoceptors in rat-1 fibroblasts release intracellular Ca^{2+}, display subtype-characteristic agonism and antagonism and exhibit an antagonist-reversible inverse concentration-response phase. *J Pharmacol Exp Ther* **293:**887–895.

Price RR, Morris DP, Biswas G, Smith MP, and Schwinn DA (2002) Acute agonist-mediated desensitization of the human α_{1a}-adrenergic receptor is primarily independent of carboxyl terminus regulation: implications for regulation of α_{1a}-AR splice variants. *J Biol Chem* **277:**9570–9579.

Resat H, Ewald JA, Dixon DA, and Wiley SH (2003) An integrated model of epidermal growth factor receptor trafficking and signal transduction. *Biophysical Journal* **85:** 730–743.

Rossier O, Abuin L, Fanelli F, Leonardi A, and Cotecchia S (1999) Inverse agonism and neutral antagonism at α_{1a}- and α_{1b}-adrenergic receptor subtypes. *Mol Pharmacol* **56:**858–866.

Roettger BF, Ghanekar D, Rao R, Toledo C, Yingling J, Pinon D, and Miller LJ (1997) Antagonist-stimulated internalization of the G protein-coupled cholecystokinin receptor *Mol Pharmacol* **51:**357–362.

Shenoy SK and Lefkowitz RJ (2003) Multifaceted roles of beta-arrestins in the regulation of seven-membrane-spanning receptor trafficking and signalling. *Biochem J* **375:**503–515.

Stanasila L, Perez JB, Vogel H, and Cotecchia S (2003) Oligomerization of the α1a- and α1b-adrenergic receptor subtypes. Potential implications in receptor internalization. *J Biol Chem* **278:**40239–40251.

Tarasova NI, Stauber RH, Choi JK, Hudson EA, Czerwinski G, Miller JL, Pavlakis GN, Michejda CJ, and Wank SA (1997) Visualisation of G-protein-coupled receptor trafficking with the aid of the green fluorescent protein. Endocytosis and recycling of cholecystokinin receptor type A. *J Biol Chem* **272:**14817–14824.

Vazquez-Prado J, Medina LC, Romero-Avila MT, Gonzalez-Esponiso C, and Garcia-Sainz JA (2000) Norepinephrine- and phorbol ester-induced phosphorylation of α_{1a}-adrenergic receptors, functional aspects. *J Biol Chem* **275:**6553–6559.

Address correspondence to: Dr. John Pediani, Autonomic Physiology Unit, Institute of Biomedical and Life Sciences, University of Glasgow, Glasgow G12 8QQ, Scotland, UK. E-mail: john.pediani@bio.gla.ac.uk